Oncogene (2015) **34,** 1853–1864

www.nature.com/onc

ORIGINAL ARTICLE

Progranulin promotes Temozolomide resistance of glioblastoma by orchestrating DNA repair and tumor stemness

I Bandey[1,2], S-H Chiou[3], A-P Huang[4], J-C Tsai[4,5] and P-h Tu[1,2]

Glioblastoma multiforme (GBM) is the most common malignant brain tumor in adults with a dismal prognosis. Current therapy of surgical removal combined with Temozolomide (TMZ) and radiation therapy only slightly prolongs the survival of GBM patients. Thus, it is essential to elucidate mechanism underlying its highly malignant properties in order to develop efficacious therapeutic regimens. In this study, we showed that progranulin (PGRN) was overexpressed in most GBM cell lines and the majority of human tumor samples. PGRN overexpression conferred GBM cells with tumorigenic properties and TMZ resistance by upregulating DNA repair (*PARP, ATM, BRCA1, Rad51, XRCC1* and so on) and cancer stemness (*CD133*, *CD44*, *ABCG2*) genes, in part via an AP-1 transcription factor, specifically cFos/JunB. Curcumin, an AP-1 inhibitor, was also found to regulate PGRN promoter activity and expression including its downstream effectors aforementioned. These data suggested a feedforward loop between PGRN signaling and AP-1. PGRN depletion significantly decreased unlimited self-renewal and multilineage differentiation and the malignant properties of GBMs cells S1R1, and enhanced their vulnerability to TMZ. In addition, S1R1 depleted of PGRN also lost the ability to form tumor in an orthotopic xenograft mouse model. In conclusion, PGRN had a critical role in the pathogenesis and chemoresistance of GBM and functioned at the top of the hierarchy of cellular machinery that modulates both DNA repair pathways and cancer stemness. Our data suggest that a new strategy combining current regimens with compounds targeting PGRN/AP-1 loop like curcumin may significantly improve the therapeutic outcome of GBM.

Oncogene (2015) **34,** 1853–1864; doi:10.1038/onc.2014.92; published online 5 May 2014

INTRODUCTION

Glioblastoma multiforme (GBM) is the most common malignant astrocytoma in adults. Despite surgery combined with radiotherapy and chemotherapy, the prognosis for GBM patients remains poor, with a median survival of ~1 year.[1,2] Thus, gaining insights into the pathways that determine the malignant nature and poor response to therapy will be instrumental for developing new therapeutic modalities. Recent studies have pointed out the resistance to Temozolomide (TMZ) through various pathways, including aberrant activation of the PI3K/Akt pathway by loss of PTEN, active base excision repair, O^6-methylguanine-DNA methyltransferase (MGMT) and so on.[3] Recently, CD133+ cells with stem cell-like features (CSCs) in GBM[4–6] were linked with an adverse prognosis,[7–11] radiochemoresistance and tumor aggressiveness.[12–15]

PGRN is a member of the cysteine-rich polypeptide family[16,17] and is present in different types of cancers and in a variety of normal tissues. It functions as a growth/survival factor in normal and pathological conditions.[18–21] In addition, overexpression of PGRN has been shown to promote resistance to various drugs, such as tamoxifen, dexamethasone, cisplatin and so on. Recent studies demonstrated that PGRN could regulate expression of stemness markers and promote chemoresistance in hepatic carcinoma.[22]

PGRN was previously identified as a human glioma-associated growth factor;[19] however, its role in GBM remains poorly characterized. A recent study found overexpression of PGRN correlated with glioma of higher grade, including GBM.[23] In this study, we present data to show that PGRN has an important role in GBM formation and its malignant property such as DNA damage repair and cancer stemness through regulating an AP-1 transcription factor.

RESULTS

Overexpression of PGRN in GBM

Previous studies demonstrated that PGRN was overexpressed in a variety of tumor types; we set out first to explore the expression of PGRN in various cell lines, including glioma (H4), GBM (U87, GBM8904, S1R1, PT3), neuroblastoma (Daoy), hepatoma (HepG1 and HepG2), breast cancer (MCF7), cervical cancer (Hela), and transformed embryonic kidney cells (HEK293). Expression of PGRN was readily detected in all cell lines, and four out of five of the human glioma/GBM cell lines except PT3 expressed high levels of PGRN protein (Figure 1a). We next tested whether similar overexpression occurred in human GBMs. Indeed, the transcript level of PGRN was significantly higher in 9 out of the 10 cases compared with cultured primary astrocytes (Figure 1b). Consistent with this, PGRN protein was also highly expressed in all seven GBM samples, which were large enough for western blot analysis (Figure 1c). In addition, PGRN protein was found to be higher in most of the 70 cases from commercial GBM tissue array by

[1]Taiwan International Graduate Program in Molecular Medicine, National Yang-Ming University and Academia Sinica, Taipei, Taiwan; [2]Institute of Biomedical Sciences, Academia Sinica, Taipei, Taiwan; [3]Department of Ophthalmology, Taipei Veterans General Hospital and National Yang-Ming University, Taipei, Taiwan; [4]Section of Neurosurgery, Department of Surgery, National Taiwan University Hospital, National Taiwan University College of Medicine, National Taiwan University, Taipei, Taiwan and [5]Center for Optoelectronic Medicine, National Taiwan University College of Medicine, National Taiwan University, Taipei, Taiwan. Correspondence: Dr P-h Tu, Institute of Biomedical Sciences, Academia Sinica, Nankang District, N701, IBMS, Academia Sinica, No.128, Sec. 2, Academia Rd. Nankang, Taipei 11529, Taiwan.
E-mail: btu@ibms.sinica.edu.tw
Received 6 August 2013; revised 10 January 2014; accepted 17 February 2014; published online 5 May 2014

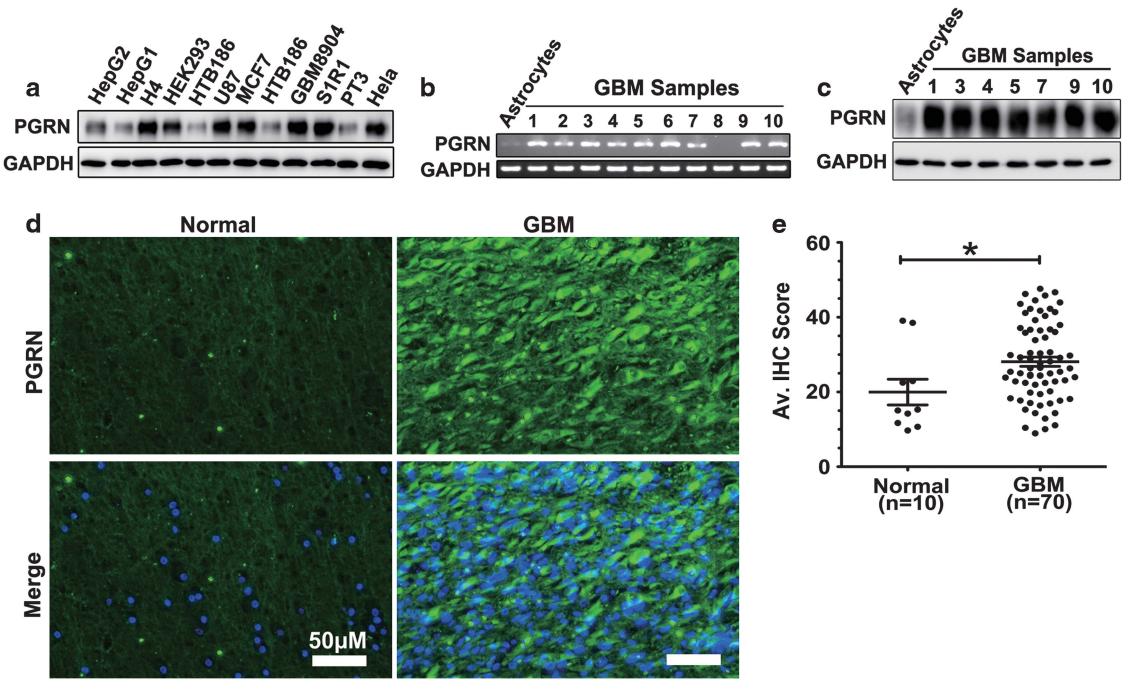

Figure 1. Overexpression of PGRN in most GBM tumors. (**a**) Western blot (WB) of various cell lines for evaluating PGRN expression. (**b**) RT–PCR and (**c**) WB of GBM tumor samples using an anti-PGRN antibody (R&D, Minneapolis, MN, USA). (**d**, **e**) Immunofluorescence staining of GBM tissue array with an anti-PGRN antibody (1:100 Abnova). The statistical analysis was performed by two-tailed *t*-test ± s.e.m. using Prism. $^*P < 0.05$ was considered statistically significant.

performing immunofluorescent staining with an anti-PGRN antibody (Figure 1d), which reached statistical significance (Figure 1e). In summary, these results validated overexpression of PGRN in GBMs.

Regulation of tumor growth by PGRN

To investigate the role of PGRN in cancer growth, the efficiency of four Sh-PGRN constructs and the rescue were evaluated by RT–PCR in S1R1 cells (Supplementary Figure S1A). The change in the PGRN protein by knockdown or overexpression was demonstrated by an immunofluorescence H4 Cell line (Supplementary Figure S1B). We showed that knockdown of PGRN caused a decrease in the growth of cells. In contrast, overexpression of PGRN increased the growth of both S1R1 (Supplementary Figure S1C) and H4 Cells (Supplementary Figure S1D).

Regulation of TMZ resistance by PGRN

TMZ resistance imposes a serious challenge on the treatment and prognosis of GBM. To examine whether PGRN was involved in this, we explored the interplay between PGRN and TMZ on cell survival and DNA synthesis ability. As shown in Figure 2a and Supplementary Figure S2A, PGRN overexpression in S1R1 cells blocked the sensitivity to TMZ (IC50 ~350 μM), whereas PGRN knockdown sensitized cells to TMZ toxicity (IC50 175 μM) compared with control cells (IC50 ~250 μM), which could be restored to that of control by coexpression of PGRN. A similar effect of PGRN on TMZ resistance was also observed in H4 cell line (Supplementary Figure S2B). Furthermore, in primary astrocytes, which lacked expression of PGRN (Figure 2b), resistance to TMZ was increased upon PGRN overexpression as shown by using an MTT assay (Figure 2c).

We next investigated the modulatory role of PGRN in DNA synthesis with or without TMZ. Overexpression of PGRN alone in S1R1 cells increased the number of EDU-labeled cells by ~24%, whereas its knockdown decreased the number by ~50% compared with control. TMZ significantly decreased the EDU-labeled cells by ~75% in PGRN knockdown cells (Figures 2d and e). In addition, PGRN overexpression significantly reversed the inhibitory effect of TMZ. Taken together, these results showed that PGRN overexpression increased DNA synthesis, consistent with its ability to enhance growth. In addition, PGRN expression has a direct bearing on cell sensitivity to TMZ genotoxicity.

Regulation of DNA damage by PGRN

TMZ-induced guanidine methylation triggers single-strand breakage in genomic DNA, and, when left un-repaired, leads to double-strand breakage (DSBs) and cell death. We examined whether PGRN was involved in cell response to DNA damage induced by TMZ.

As shown in Figures 3a and b, 250 μM TMZ treatment increased the number of phosphorylated H2AX (pH2AX) foci (indicative of DSBs) in S1R1 cells by 3.7-fold, while PGRN overexpression blocked their formation. In contrast, TMZ markedly increases the number by ~18-fold in PGRN knockdown cells. A corresponding change in the level of pH2AX was confirmed by western blot (Figures 3c and d). The correlation between the pH2AX level and the change in PGRN expression was also observed in H4 cell line (Supplementary Figures S2C and F). We also demonstrated that PGRN knockdown sensitized S1R1 cells in a dose-dependent manner (Supplementary Figure S2G).

To assess the extent of DNA damage induced by TMZ, we performed the alkaline comet assay in S1R1 cells. TMZ (250 μM) treatment or PGRN knockdown alone each induced short DNA tails in a subset of cells. However, TMZ significantly increased the percentage of cells with long comet tails in PGRN knockdown cells. On the contrary, PGRN-overexpressing cells demonstrated resistance to DNA damaging effect of TMZ (Figures 3e and f). Taken together, these results showed that knockdown of PGRN rendered cells prone to DNA damage by TMZ probably on account of the faulty DNA repair system.

Previous studies showed that TMZ promoted G2/M arrest in various cell lines.[24] Our cell cycle analysis by flow cytometry

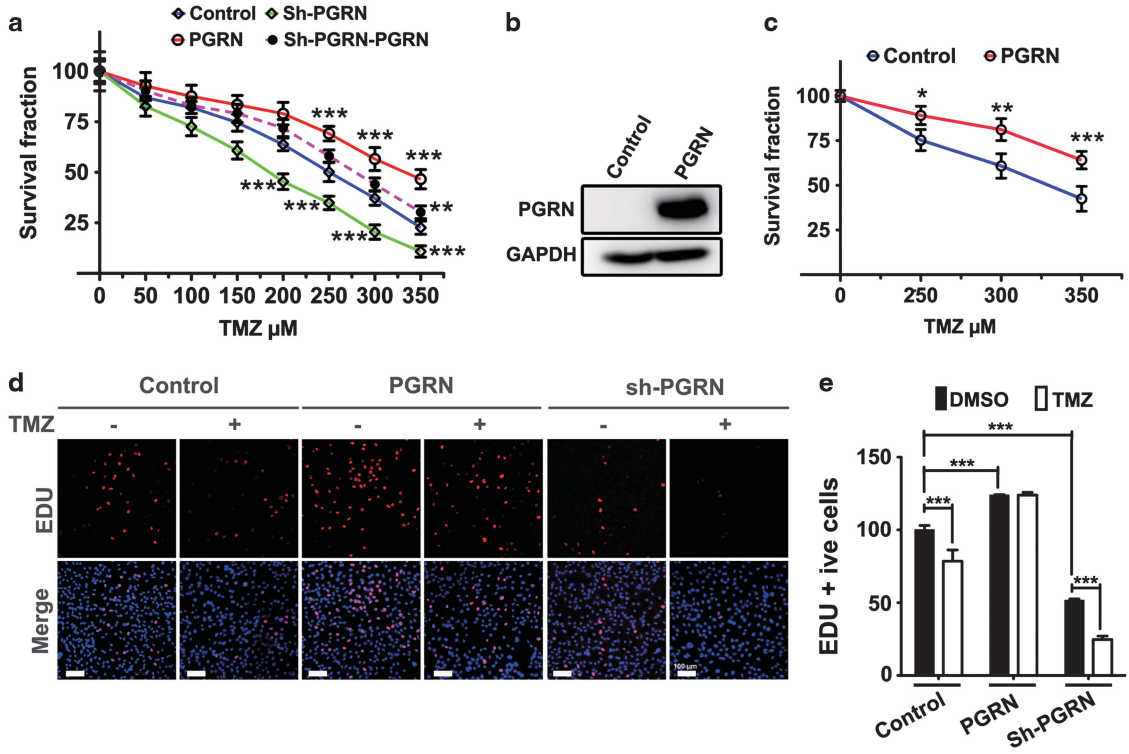

Figure 2. Role of PGRN in TMZ resistance and/or EDU labeling in S1R1 cells and primary astrocytes. (**a**) Survival percentage of S1R1 cells as a function of TMZ concentration by using an MTT assay. The assay was performed in triplicates and repeated three times. Statistical analysis was done by two-way ANOVA with Bonferroni post test (**b**) Western blotting of primary mouse astrocytes with or without PGRN overexpression. No endogenous PGRN was detected in astrocytes. (**c**) Survival percentage of control and PGRN-overexpressing primary astrocytes upon TMZ treatment. (**d**) Confocal images and (**e**) quantitation of EdU-labeled S1R1 cells overexpressing PGRN (PGRN) or infected with Sh-PGRN knockdown viral particles with dimethylsulfoxide (DMSO) (−) or TMZ (+, 250 μM). Scale bar, 100 μM. Note: the obvious attenuation of EdU-labeled cells in Sh-PGRN knockdown cells with or without TMZ. Statistical analysis: two-way ANOVA with Bonferroni post test. * < 0.05, ** < 0.01, *** < 0.001.

showed that control and PGRN-overexpressing S1R1 cells were able to overcome G2/M arrest induced by 250 μM TMZ in 48 h, indicating an intact DNA repair system. In contrast, PGRN-depleted cells failed to recover from the TMZ-induced G2/M arrest. In addition, a concomitant increase in SubG1 population, indicative of cell death, was clearly detected (Figure 3g and Table 1). Notably, PGRN overexpression in PGRN-depleted cells was able to rescue the cells from G2/M arrest. RT–PCR studies showed TMZ treatment induced an upregulation of pro-survival Bcl-2 in control cells, but pro-death GADD45, instead, in the PGRN-depleted cells (Figure 3h). These data showed that PGRN was able to protect cells against TMZ challenge by upregulating pro-survival gene and maintaining cell cycle integrity.

Role of PGRN in clonogenic and migration ability

To explore the role of PGRN in unlimited division of cells, a clonogenic assay was conducted. Our data indicated that PGRN overexpression alone increased colony formation by 22%; knockdown of PGRN resulted in a marked drop in this ability by ~68%. TMZ impaired the ability of S1R1 to form colony by 40%, and by >90% in the presence of PGRN deficiency. The attenuated colony formation by PGRN knockdown in the presence or absence of TMZ could be rescued by coexpression of PGRN (Figures 4a and b).

Similarly, PGRN knockdown or TMZ treatment impaired the wound healing capability of S1R1 cells, which could be further retarded when they were combined (Figures 4c and d). PGRN coexpression rescued cells from the toxicity of TMZ and/or PGRN knockdown.

Anchorage-independent cell growth is an important hallmark of tumorigenicity. We next evaluated the interplay of PGRN and TMZ in this property by using a soft agar assay. Control S1R1 cells efficiently formed colonies in 3 weeks, and TMZ treatment decreased the size of colonies by ~47%. Knockdown of PGRN caused a severe diminution in the colony size by ~75%, which could be effectively rescued by coexpression of PGRN. Again, PGRN knockdown plus TMZ decreased the colony size by 90%, which was also partially rescued by co-expression of PGRN (Figures 4e and f). Taken together, PGRN regulated multiple parameters essential for tumorigenesis and protected cells against TMZ-induced toxicity.

Regulation of stemness by PGRN

Cancer stemness has been recognized as an important factor of resistance to radiochemotherapy. To explore the role of PGRN in maintaining this, we performed RT–PCR of GBM samples and found that, compared with astrocytes, the majority of GBM samples expressed high levels of CD133 and ATP-binding cassette subfamily G member 2 (ABCG2) mRNA, two important glioma stemness markers, which strongly correlated with the level of PGRN expression (Figure 5a).

In S1R1 cells, $CD133^+$ subpopulation dropped from 27 to 3% by PGRN knockdown and increased to 57% upon PGRN overexpression. Notably, PGRN overexpression in PGRN knockdown rescued the CD133 subpopulation to 43.8% as shown by flow cytometry analysis (Figure 5b). In addition, the levels of transcripts and proteins of several glioma stemness markers, including CD133, ABCG2 and CD44, increased with PGRN overexpression and decreased with PGRN knockdown, which were rescued by coexpression of PGRN (Figures 5c and d).

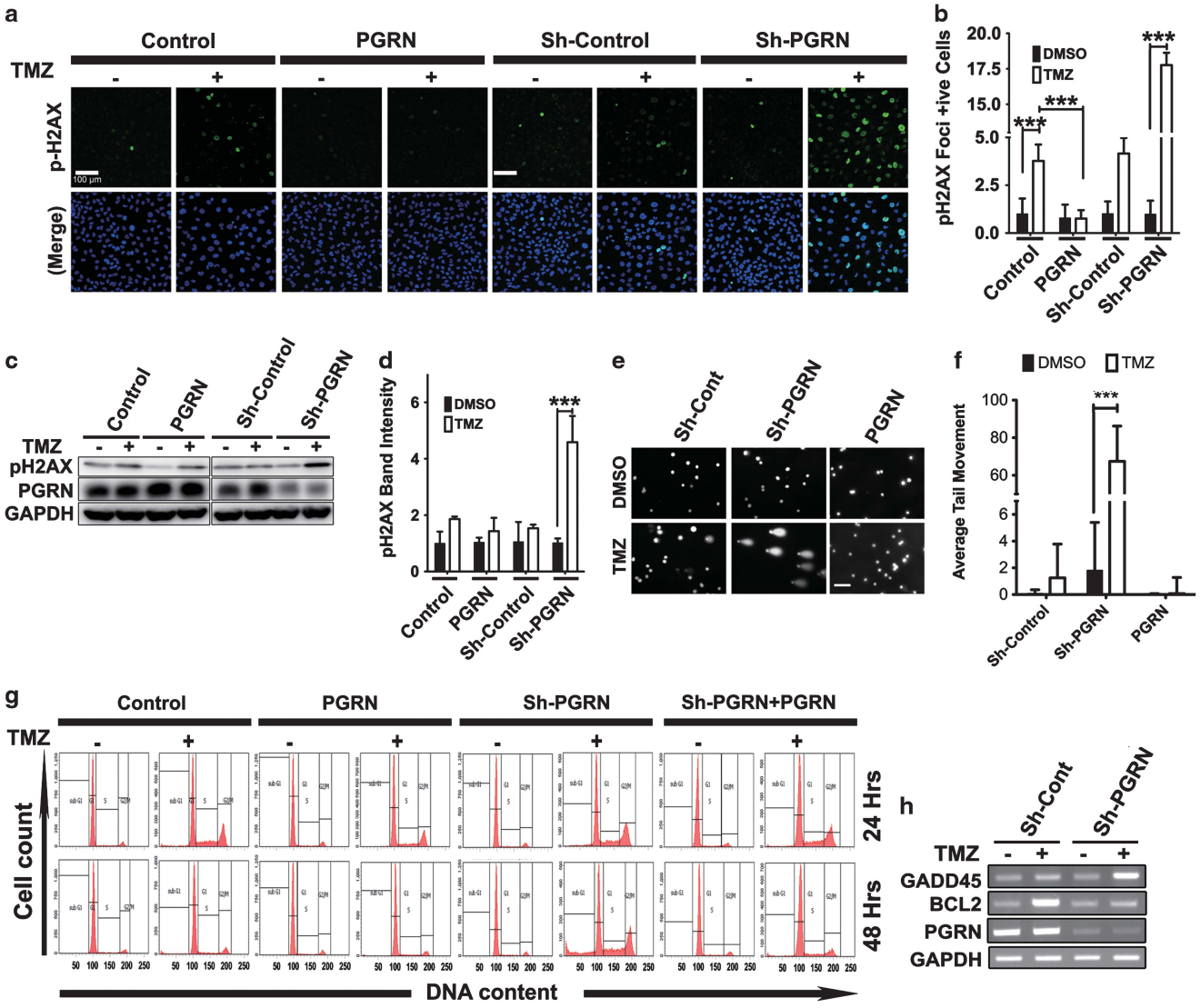

Figure 3. Role of PGRN in TMZ-induced DNA damage. (**a**) Confocal images of S1R1 cells infected with treated as indicated. Scale bar, 100 μm. Cells were stained with an anti-pH2AX antibody (green) and DAPI (blue). (**b**) Quantitation of number of cells with pH2AX foci. About 50 cells per sample were manually counted. (**c**) WB and (**d**) corresponding quantitation of cell lysates as indicated with an anti-pH2AX antibody. Note: significant increase in the pH2AX in TMZ and TMZ/Sh-PGRN cells. (**e**) DNA damage visualized by using an alkaline Comet assay. (**f**) Quantitation of the tail length. Around 50 comets/sample were scored. (**g**) Representative cell cycle histograms showing S1R1 cells treated as indicated. Note: PGRN knockdown (Sh-PGRN) cells with clear G2/M arrest and enhanced SubG1 debris in the presence of 250 μM TMZ at 48 h. PGRN overexpression (PGRN) rescues Sh-PGRN cells from TMZ-induced G2/M arrest. (**h**) Representative RT–PCR results of Bcl-2 and GADD45 from cells treated as indicated. The experiment was performed three times. Statistical analysis: two-way ANOVA with Bonferroni post test. *** < 0.001.

Next, we sorted parental S1R1 cells into $CD133^+$ and $CD133^-$ subpopulations using a PE-conjugated anti-CD133 antibody and found that high PGRN expression correlated with $CD133^+$ subpopulation (Figure 5e).

Sphere formation is an established property for CSCs. It was clear that the spheres formed by S1R1 cells depleted of PGRN were significantly smaller than those formed by control (Figures 5f and g). RT–PCR from these spheres showed that the level of CD133 transcript remained low in PGRN knockdown spheres (Figure 5h). Consistently, the surface CD133 expression on the surface of PGRN knockdown spheres was also lower than that of control spheres as shown by flow cytometry (Supplementary Figure S3A).

The expression of the stemness marker ABCG2 was also tightly associated with the level of PGRN (Figures 5a, c and d). ABCG2 marks a subpopulation of CSCs, designated side population (SP), which can be assayed by using the Hoechst exclusion test. PGRN overexpression significantly increased the SP from 2.6 to 10.3% in S1R1 (Figure 5i), and H4 cell line as well (Supplementary Figure S3B). Altogether, these data clearly demonstrated the important role of PGRN in regulating the stemness of GBM.

PGRN promoting TMZ resistance through regulating cancer stemness

To further study the mechanism PGRN used to promote TMZ resistance, S1R1 cells were continuously cultured at high dose (1000 μM) of TMZ for 1 month. Four subclones were isolated. Interestingly, all of them expressed much higher level of PGRN and of stemness markers CD133, CD44 and ABCG2 than their paternal cells (Figure 5j). The MTT assay revealed that $CD133^+$ cells were more resistant to TMZ than $CD133^-$ cells. Interestingly,

Table 1. Cell cycle distribution

	DMSO	*TMZ*	*DMSO*	*TMZ*	*DMSO*	*TMZ*	*DMSO*	*TMZ*
	Control		*PGRN*		*Sh-PGRN*		*Sh-PGRN +PGRN*	
24 h								
SubG1	0.6	5.9	0.5	2.5	0.5	5.6	0.5	3.8
G1	82.8	48.5	83	62.5	84.1	47.9	84.8	55.5
S1	8.8	21.8	7.8	13.6	6.7	17.6	6.6	17.4
G2M	7.9	23.8	8.8	21.4	8.6	29	7.9	23.3
48 h								
SubG1	1.2	6.8	1.1	3.7	0.6	22	0.7	5
G1	86	73.4	84.7	79.5	85.4	36.6	85.3	73.8
S1	6	9.1	6.3	8	6.2	18.9	6	9.8
G2M	6.8	10.8	7.7	8.7	7.7	22.4	8	11.4

Abbreviations: DMSO, dimethylsulfoxide; PGRN, progranulin; TMZ, Temozolomide.

PGRN knockdown rendered the $CD133^+$ subpopulation as vulnerable as the $CD133^-$ to TMZ. On the contrary, PGRN overexpression also made $CD133^-$ subpopulation behave like $CD133^+$ (Figure 5k). Taken together, our data suggested PGRN to be a major determinant for stemness property, which could at least partially account for its role in TMZ resistance.

Role of PGRN in unlimited self-renewal and differentiation

CSCs possess unlimited self-renewal potential demonstrated via limited dilution upon multiple rounds of passages. To investigate whether PGRN had a pivotal role in this property, S1R1 control or PGRN knockdown cells were grown at limited densities of 1, 10 and 50 cells/well in an ultralow attachment 96-well dish. PGRN knockdown cells suffered attenuation in the self-renewal ability (Figure 6a). In addition, the control S1R1 formed more spheres with passages, whereas the spheres formed by PGRN knockdown cells failed to increase or gradually decreased with passages (Figure 6b). These results demonstrated that PGRN had an important role in unlimited self-renewal of CSCs.

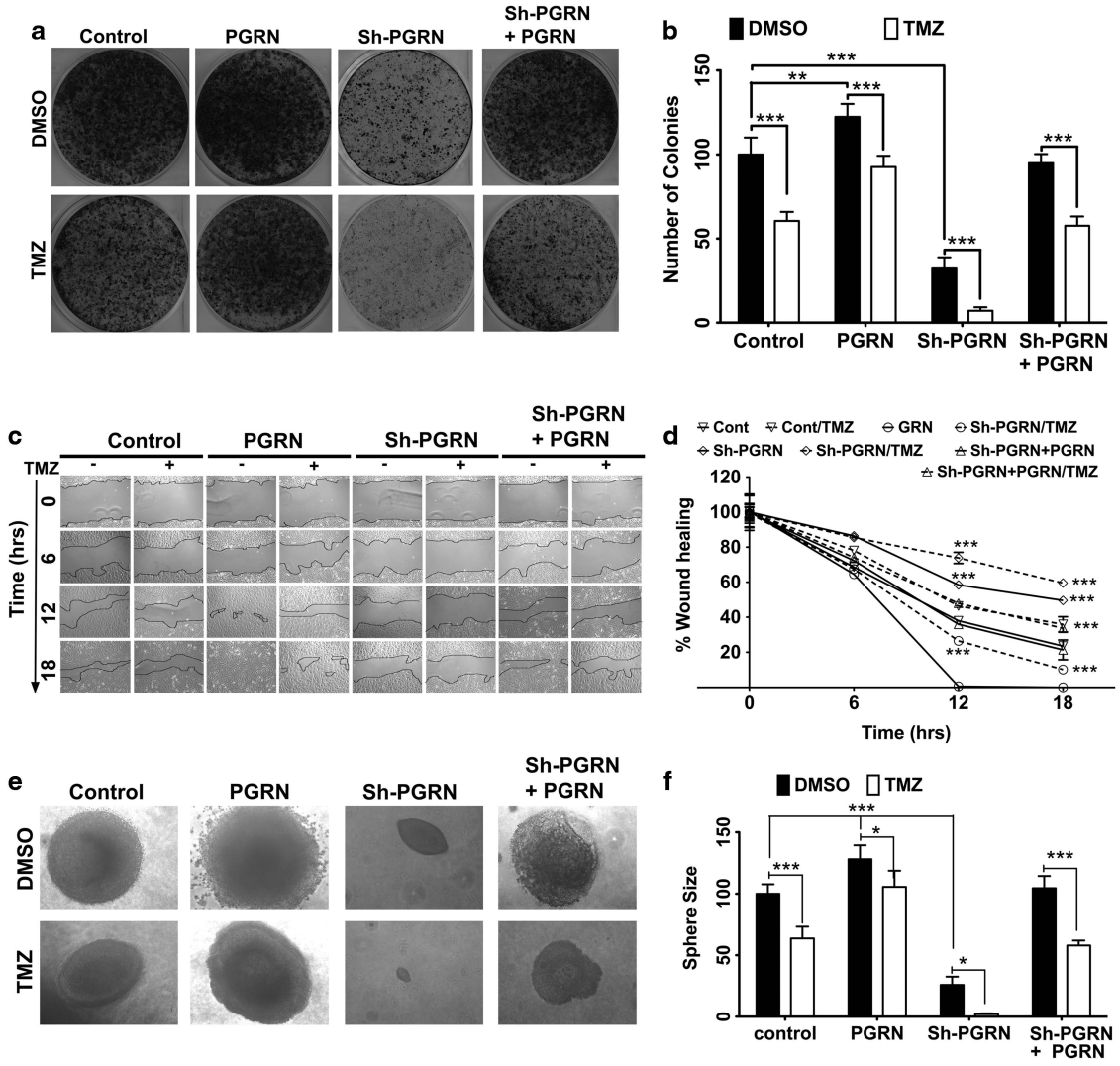

Figure 4. Attenuation of various malignancy properties by PGRN knockdown: S1R1 cells overexpressing PGRN, infected with Sh-PGRN lentiviral particles (Sh-PGRN) or with rescue (Sh-PGRN/PGRN) treated with 250 μM TMZ (+) or DMSO (–). (**a**, **b**) Pictures and quantitation of colonies formed after 3 weeks. (**c**, **d**) Wound healing assay and quantitation of S1R1 cells treated as indicated at specified time points. (**e**, **f**) Pictures of colonies formed in soft agar and quantitation. Statistical analysis: two-way ANOVA with Bonferroni post test. * < 0.05, ** < 0.01, *** < 0.001.

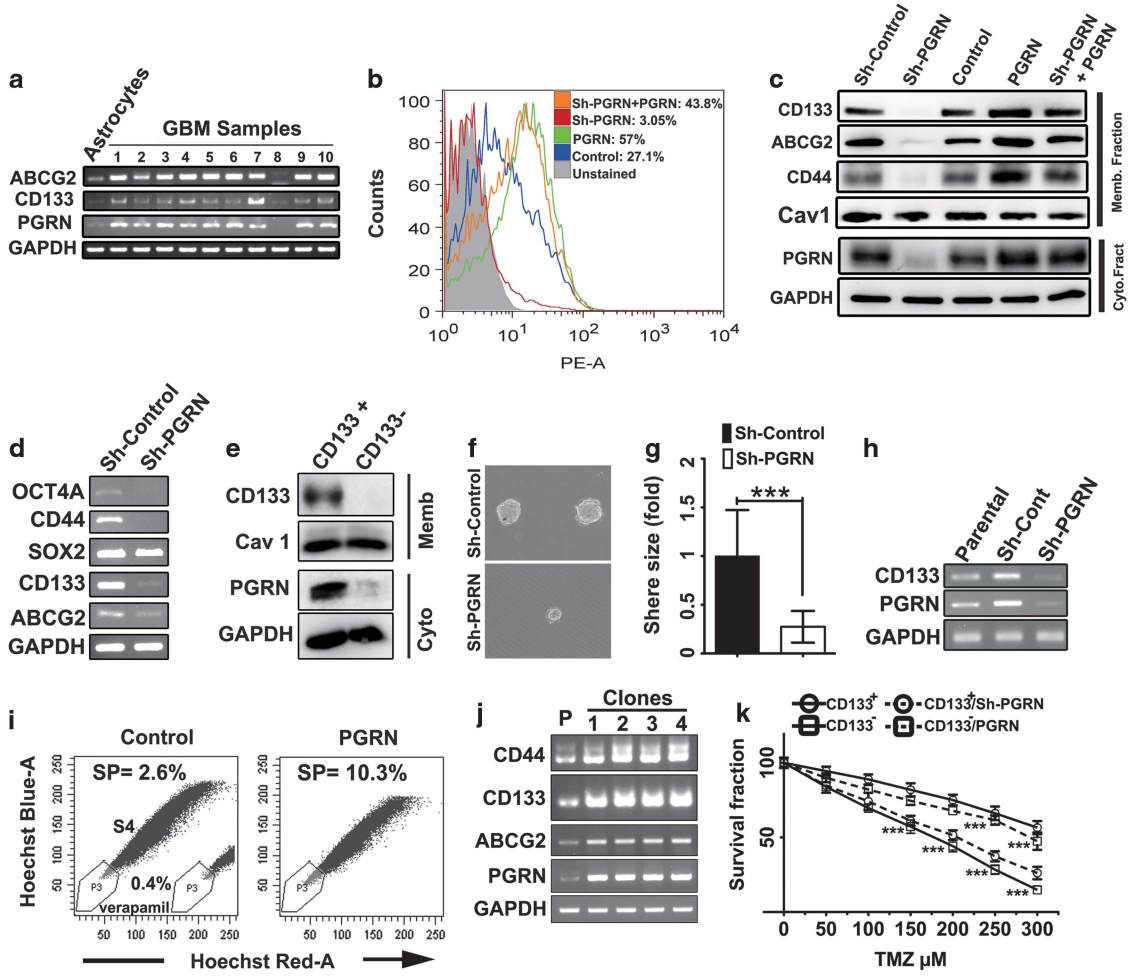

Figure 5. Regulation of stem cell markers by PGRN. (**a**) RT–PCR results of GBM tumor samples vs astrocytes to show increased expression of ABCG2, CD133 and PGRN. (**b**) Quantitation of $CD133^+$ subpopulation in S1R1 cells treated as indicated by flow cytometry using an anti-$CD133^-$ PE antibody. Note: attenuation of $CD133^+$ subpopulation by PGRN knockdown (Sh-PGRN, red curve), which could be rescued by coexpression of PGRN (Sh-PGRN+PGRN, orange curve). (**c**) WB and (**d**) RT–PCR of stemness markers in S1R1 cells treated as indicated. Loading controls used: caveolin 1 (membrane fraction) and GAPDH (cytoplasmic fraction). (**e**) WB of flow cytometry sorted $CD133^+$ and $CD133^-$ subpopulation. Note: PGRN was primarily detected in $CD133^+$ subpopulation. (**f**, **g**). Phase contrast image and quantitation of stem cell sphere formation by S1R1 control and PGRN knockdown cells. Note: a reduction in sphere size by PGRN knockdown. Statistics were done with Student's *t*-test. (**h**) RT–PCR of stem cell spheres formed by parental cells, cells infected with Sh-control or Sh-PGRN. CD133 expression remained low in spheres by Sh-PGRN knockdown cells. (**i**) A Hoechst exclusion assay to detect side population of control and PGRN-overexpressing S1R1 cells, by flow cytometry. Inset: results of verapamil-treated cells treated with ABCG2 blocked as negative control. (**j**) RT–PCR of PGRN and stem cell markers from four TMZ-resistant subclones selected by 1000 μM TMZ treatment for 1 month. (**k**) An MTT assay of sorted $CD133^+$ subpopulation ($CD133^+$, solid line with circle), $CD133^-$ subpopulation ($CD133^-$, solid line with square), $CD133^+$ subpopulation infected with Sh-PGRN lentivirus ($CD133^+$/Sh-PGRN, dashed line with circle) and $CD133^-$ subpopulation overexpressing PGRN ($CD133^-$/PGRN, dashed line with square) Statistics were performed by two-way ANOVA with Bonferroni post test. *** < 0.001.

Next, we examined whether PGRN regulated the differentiation of these stem cells. As expected, the spheres with PGRN depleted cells exhibited lower PGRN and CD44 compared with control (Figure 6c). Under 5% FBS, cells of the sphere migrated to form a monolayer on coverslips (Phase, Figure 6c), some of which expressed the astrocytic marker GFAP and neuronal marker MAP2 (Figure 6c). Interestingly, PGRN knockdown significantly decreased the percentage of the GFAP+ or MAP2+ subpopulation (Figure 6d). These results showed that PGRN might be involved in the regulation of astrocytic and neuronal phenotypes of GBM.

Role of PGRN in DNA damage repair

O^6-methylguanine (O^6MeG) is a DNA adduct important for TMZ toxicity, which can be repaired by MGMT. However, knockdown of PGRN did not change the level of MGMT in S1R1 cells (Supplementary Figure S4A), suggesting that PGRN modulated TMZ toxicity by an MGMT-independent mechanism. Given enhanced DSBs in cells depleted of PGRN, we investigated whether DNA repair system was governed by PGRN signaling. Indeed, the transcripts of DNA repair machinery, such as ataxia telangiectasia mutated (ATM), *Rad51*C&D, *XRCC1* and *PARP*, positively correlated with the level of PGRN in S1R1 cells (Figure 7a). Expression of these molecules increased upon TMZ challenge, which was significantly attenuated in PGRN-depleted S1R1 cells. In contrast, the transcript of DNA-dependent protein kinase, catalytic subunit (DNA-PKcs), which regulates non-homologous end joining (NHEJ) repair, failed to change with PGRN (Figure 7a). Inhibition of DNA-PKcs with NU7026 did not significantly enhance the TMZ sensitivity of control or PGRN

knockdown S1R1 cells (Supplementary Figure S4B), excluding the NHEJ machinery from the PGRN-mediated DSB repair system under TMZ challenge.

Next, we examined the expression of genes involved in DNA repair in human GBM samples. A general correlation existed between mRNA of PGRN and transcripts of DNA repair genes, particularly for *ATM* and *PARP*, which showed striking correlation (Figure 7b). PGRN overexpression increased, whereas its knockdown resulted in a subsequent decrease in *PARP* expression as shown by western blot analysis (Figure 7c). In addition, PGRN depletion decreased the survival of S1R1 under TMZ treatment, and inhibition of *PARP* by its inhibitor ABT888 further potentiated the effect, while a *PARP* inhibitor did not further sensitize control or PGRN-overexpressing cells to TMZ (Figure 7d). This indicated that *PARP* inhibition together with HR pathway deficiency synergistically sensitized cells to TMZ. Similar changes were also observed in the H4 cell line (Supplementary Figure S4C).

PGRN mediating TMZ toxicity through AP-1

Previous studies have shown that activator protein (AP-1) complex has a central role in tumorigenesis and drug resistance in glioma.[25] To gain more mechanical insight into the PGRN-mediated pathway, we tested whether PGRN regulated an AP-1 transcription factor. In S1R1 cells, PGRN overexpression increased and PGRN knockdown decreased the expression of cFos and JunB transcripts (Figure 7e) and proteins (Figure 7f), but not other AP-1 components such as JunD. The PGRN knockdown yielded complementary changes. In H4 cells, PGRN positively regulated the expression of transcripts (Supplementary Figure S4D) and proteins (Supplementary Figure S4E) of FosB and JunB. cFos, JunB and FosB were also highly expressed in 9/10 human GBM samples and strongly correlated with expression of PGRN (Figure 7g). Intriguingly, in S1R1 cells, overexpression of PGRN or coexpression of cFos and JunB in both control and PGRN-depleted cells increased the expression of DNA repair gene *ATM*

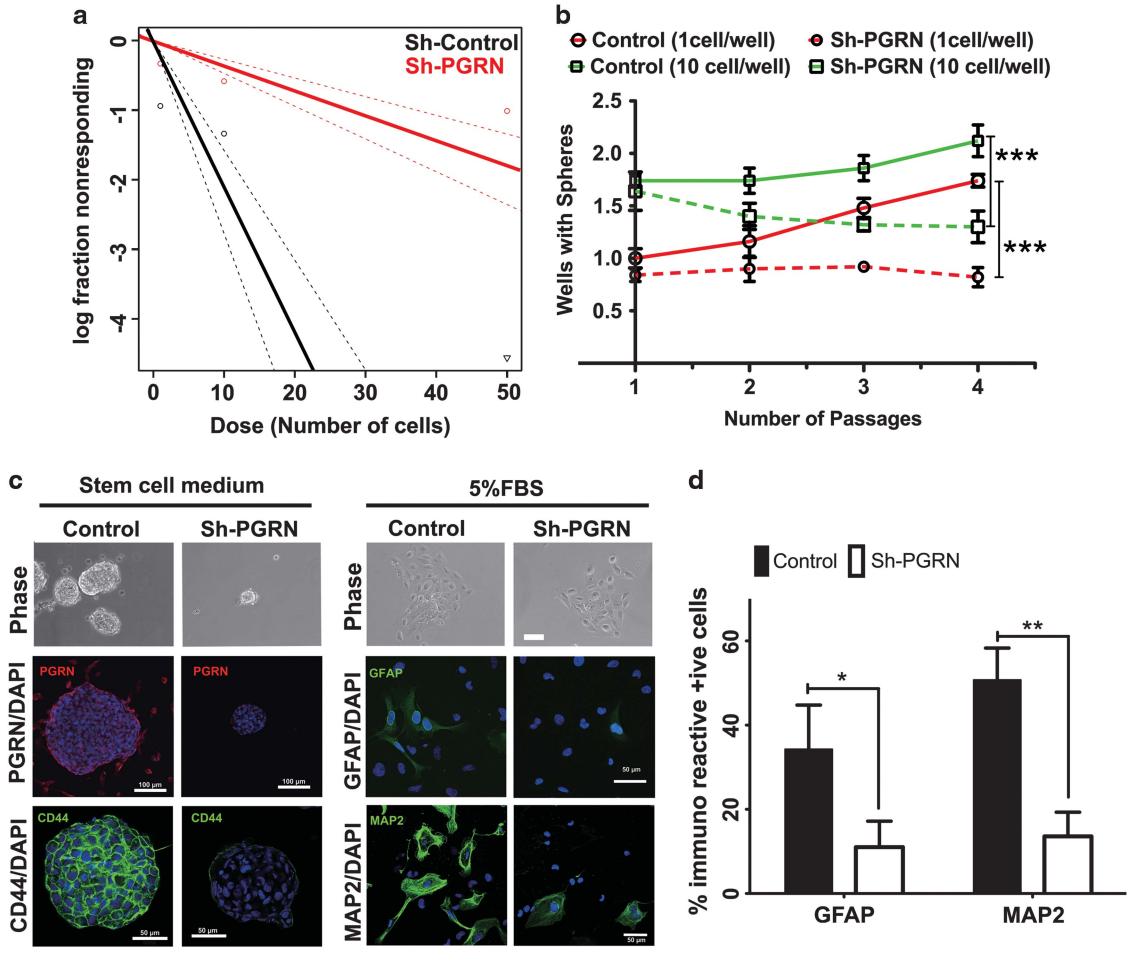

Figure 6. Regulation of unlimited self-renewal and differentiation potential by PGRN. (**a**) Limiting dilution assay as linear regression curves to determine the frequency of colony formation by control vs PGRN knockdown S1R1 cells plated at dilution of 1,10 and 50 cells/well. (**b**) Number of wells containing at least one sphere at dilution of 1 or 10 cells/well plotted against passage number. Note: the frequency of Sh-Control at one cell/well (Red solid line) or 10 cells/well (Green solid line) increased, while that of Sh-PGRN at one cell/well (dashed red line) or 10 cells/well (green dashed line) remained unchanged or progressively diminished. Statistical analysis was performed by two-way ANOVA with Bonferroni post test. (**c**) Phase contrast (Phase) and confocal images of stem cell spheres formed in stem cell medium or monolayer of differentiated cell sheet in 5% FBS by Sh-Control and Sh-PGRN S1R1 cells (Scale bar, 100 μm). The spheres formed by PGRN knockdown (Sh-PGRN) S1R1 cells were not only smaller in size but also had lower CD44 and PGRN than those formed by Sh-control (Control) cells. Expressions of GFAP (astrocyte marker) and MAP2 (neuronal marker) were noted in both Sh-Control and Sh-PGRN S1R1 cells by immunofluorescent stainings. (**f**) Quantitation of immunoreactive-positive cells over 10 random fields. Percentage of cells expressing GFAP or MAP2 was significantly decreased by Sh-PGRN knockdown. Statistical analysis was performed by two-way ANOVA with Bonferroni post test. * < 0.05, ** < 0.01, *** < 0.001.

and stemness marker CD133 (Figure 7h). Furthermore, while PGRN depletion sensitized S1R1 cells to TMZ toxicity, co-expression of cFos and JunB fully restored the resistance of PGRN-depleted cells to the control level. Thirty micromolars of curcumin, an AP-1 inhibitor, attenuated the TMZ resistance in both control and PGRN knockdown cells by using an MTT assay (Figure 6i). Similar effects were also observed in the H4 cell line (Supplementary Figure S4F). Taken together, these results clearly showed that PGRN mediated TMZ toxicity by upregulating genes involved in stemness and DNA repair through an AP-1 transcription factor.

PGRN overexpression partially regulated by an AP-1 transcription factor

Given the important role of PGRN overexpression in GBM pathogenesis, an effort to identify potential transcription factors underlying PGRN overexpression was attempted using a PGRN promoter-luciferase reporter assay. We found by reporter assay a critical region that governed PGRN promoter activity resided between −151 and −161, within which AP-1, CEBP and XBP1 binding sites were predicted with PROMO version 3.0.2 (http://alggen.lsi.upc.es/cgi-bin/promo_v3/promo/promoinit.cgi?dirDB=TF_8.3). Mutating the AP-1 and CEBP sites entirely eliminated the

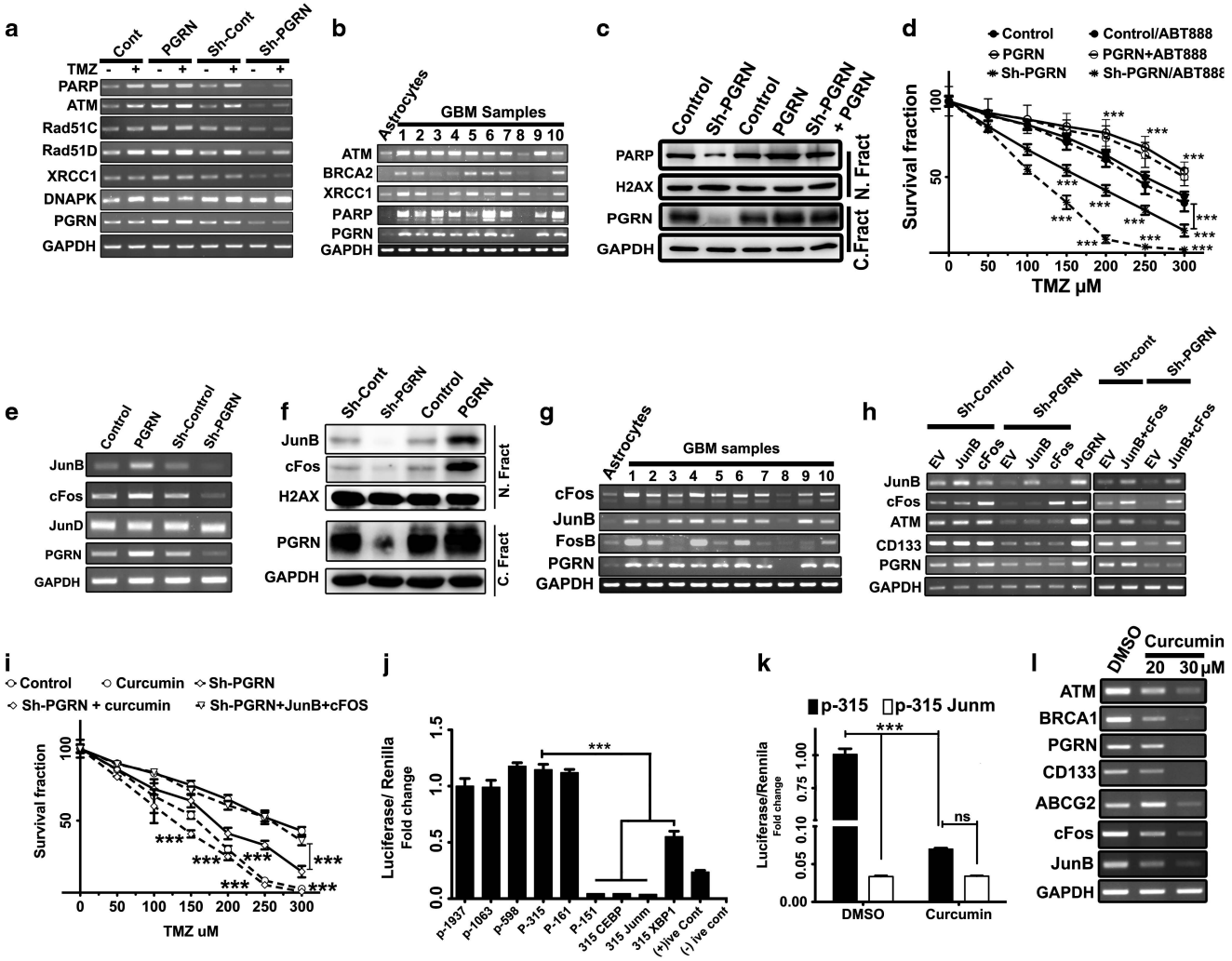

Figure 7. Regulation of expression of DNA repair genes by PGRN/AP-1. (**a**) RT–PCR assays of the DNA repair system in (**a**) S1R1 cells overexpressing PGRN (PGRN) or depleted of PGRN (Sh-PGRN) vs control and in (**b**) Human GBM tumor samples vs astrocytes. (**c**) WB of S1R1 cells showing expression of *PARP* in relation to PGRN knockdown (Sh-PGRN), overexpression (PGRN) and rescue (Sh-PGRN+PGRN). Note: a positive correlation of *PARP* expression with PGRN. (**d**) TMZ resistance by using an MTT assay of S1R1 cells treated as indicated. ABT888 (a *PARP* inhibitor) used at 20 µM. (**e**) RT–PCR and (**f**) WB of S1R1 cells treated as indicated to detect changes in cFos and JunB, two AP-1 components. Note: a positive correlation between PGRN and cFos/JunB. (**g**) Correlation of PGRN and AP1 components in human GBM samples vs astrocytes by RT–PCR. Note: an excellent correlation between PGRN and cFos/JunB. (**h**) Regulation of CD133 (stemness marker) and *ATM* (DNA damage repair marker) by cFos/JunB in samples as indicated. Note: a positive correlation of these genes with c-Fos/JunB coexpression, but not with expression of either one alone. (**i**) Attenuation of TMZ resistance by 30 µM curcumin pretreatment by MTT assays using control S1R1 cells treated with TMZ (solid line with circle), pretreated with curcumin 6 h before adding TMZ (Dashed line with circle), Sh-PGRN cells treated with TMZ (Solid line with diamond) or pretreated with 30 µM curcumin 6 h before adding TMZ (dashed line with diamond) and Sh-PGRN cells co-overexpressing cFos/JunB followed by TMZ (dashed line with inverted triangle). The assays were done in triplicates and repeated three times. Statistical analysis was done by two-Way ANOVA. (**j**) PGRN Promoter-luciferase Assay. Note: a marked difference between −161 and −151. Mutation at predicted binding site for cJun (Junm), CEBP (CEBP) or XBP1 (XBP1) was done with PGRN promoter containing sequence from −1 to −315 (p-315). (**k**) Inhibition of PGRN promoter activity by curcumin. (**l**) Inhibition of expression of PGRN and downstream genes by curcumin at indicated doses. *** < 0.001.

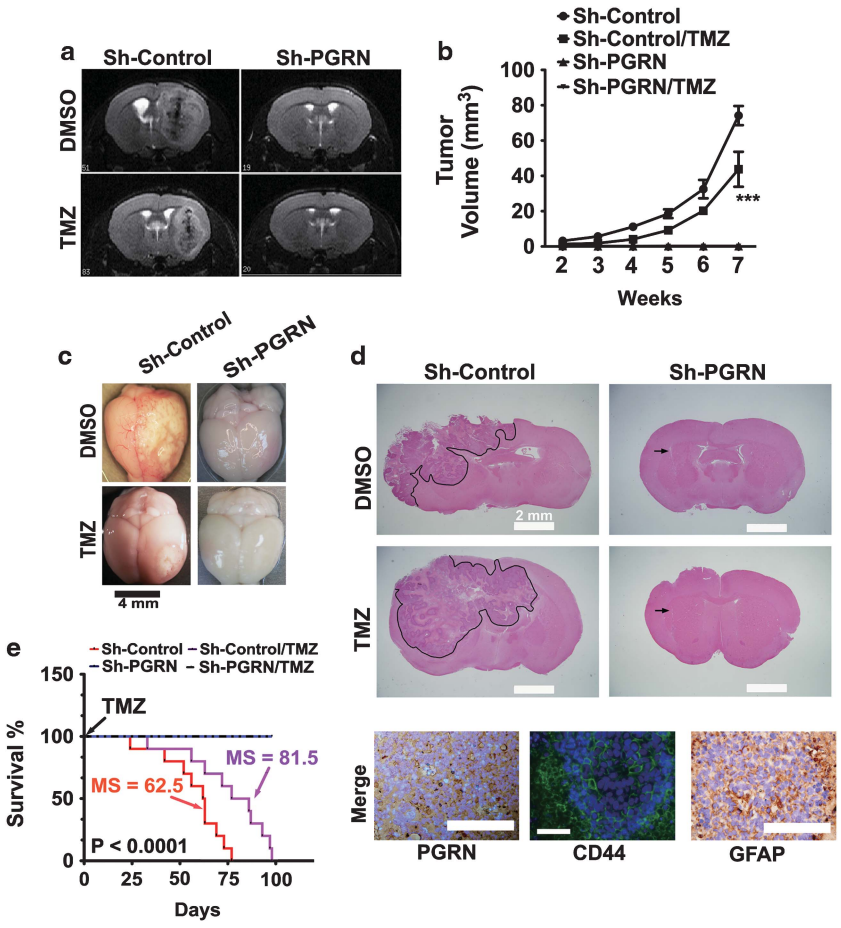

Figure 8. Inhibition of tumor growth by PGRN depletion in an orthotopic mouse model. (**a**) MRI images of intracerebral tumors formed by S1R1 cells 8 weeks after injection into the mouse brain. TMZ or DMSO was given intraperitoneally. (**b**) Growth curve of intracerebral tumors treated as indicated by MRI. (**c**) Gross examination of tumors treated as indicated. No tumor formed by PGRN-depleted cells was visible on the cortical surface (Scale bar, 4 mm). (**d**) Images of H&E-stained mouse brain sections to reveal tumor inside the brain. Note: a large tumor (encircled) formed by the Sh-control cells in mouse treated with DMSO or TMZ treatment. The needle tract (arrows) without clear tumor was detected in mouse injected with Sh-PGRN virus-infected S1R1 cells (Scale bar, 2 mm). Tumors formed by Sh-control cells in the mouse brain were evaluated for CD44 expression by immunofluorescence (Scale bar, 50 μm), PGRN and GFAP by immunohistochemistry (Scale bar, 100 μm). (**e**) Kaplan–Meier survival curve of mice treated as indicated. Note: mice receiving Sh-PGRN-treated cells with DMSO or TMZ survived through tested period.

promoter activity, but XBP1 mutation decreased the activity by ~50% (Figure 7j). Curcumin treatment inhibited the promoter activity as the AP-1 site mutation (Figure 7k). To further validate the role of AP-1 in PGRN expression, we found curcumin treatment indeed reduced expression of PGRN and its downstream effectors of the DNA repair system (Figure 7l). Taken together, these results showed that PGRN expression was at least partially regulated by an AP-1 transcription factor.

Inhibition of tumor growth by PGRN knockdown in an orthotopic model

To validate the role of PGRN in GBM pathogenesis *in vivo*, we used an orthotopic xenograft mouse model. MRI studies showed that S1R1 cells injected into the striatum were able to form large tumors in mouse brains; TMZ administration only mildly decreased tumor size. In sharp contrast, PGRN knockdown eliminated the ability of S1R1 cells to develop into detectable tumors with or without TMZ treatment (Figures 8a and b). The gross examination of mouse brain revealed that tumors were visible on the surface of control and TMZ-treated mouse brains, but not seen in mice injected with PGRN-depleted cells with or without TMZ (Figure 8c). The histopathologic examination of the control tumors showed features characteristic of human GBM, including highly malignant cytology and geographic necrosis; expression of PGRN, CD44 and GFAP was observed throughout the tumors (Figure 8d). All control mice became death-imminent within 90 days post injection (mean survival = 62.5 days), and TMZ-treated mice, within 100 days (mean survival 81.5 days) (Figure 8e). None of the mice injected with the PGRN-depleted cells died within the tested time period. These data clearly underlined the importance of PGRN in the pathogenesis of GBM *in vivo*.

DISCUSSION

In this study, we showed that PGRN had an important role in the pathogenesis of GBM through regulating DNA repair systems and cancer stemness, two key components of tumorigenesis and chemoradiation resistance. Previous studies illustrated the AKT and MAPK signaling pathways in PGRN-mediated tumorigenesis;[26,27] this current study has further extended the importance of PGRN in GBM.

GBM is notorious for its resistance to current therapeutic modality. Here, we demonstrated that the PGRN-mediated DNA

repair system and cancer stemness likely accounted for the treatment resistance. *PARP* is involved in repair of SSBs; in the absence of *PARP*, the replication fork stalls during replication and DSBs accumulate. Then HR or NHEJ mechanism or both are required for repair of the DSBs. We found that PGRN knockdown diminished *PARP* and the HR pathway. Previous studies suggested the benefits to combine TMZ with a *PARP* inhibitor.[28] Conceivably, this strategy may be less effective in DNA repair system-prolific tumors. Given its modulatory role in the PGRN signaling pathway, and the ability to pass the blood–brain barrier,[29] our study indicates that TMZ/curcumin may serve as a better combinational regimen than the TMZ/*PARP* inhibitor against GBM.

The identification of CSCs has created a major paradigm shift in our understanding of carcinogenesis and chemotherapy. In this study, we found that PGRN regulated $CD133^+$ CSCs and their property, and that this stemness contributed to the TMZ-resistance. Besides CD133, ABCG2 was also regulated by PGRN. ABCG2 was shown to be upregulated in both glioblastoma vessels and parenchymal tissue,[30] indicative of its role in conferring drug resistance to GBM. Although TMZ is not a direct substrate of ABCG2, TMZ was reported to increase MGMT expression and aggressiveness of $ABCG2^+$ SP cells.[31] Hypoxia has been shown to have a vital role in GBM progression and tumor stem cell maintenance.[32] Moreover, both PGRN and ABCG2 have been shown to be upregulated under hypoxia[33] and promote cell survival.[34] Given our results that, PGRN regulated ABCG2, it is tempting to speculate that PGRN may promote sturdiness to GBM under hypoxia via ABCG2. PGRN also regulated CD44, which enhanced GBM progression and resistance to TMZ.[35] Furthermore, PGRN regulated the unlimited self-renewal and multilineage differentiation potential. Taken together, PGRN has a vital role in GBM stemness, which may in part contribute to the high malignancy of GBM.

An AP-1 transcription factor has been previously shown to have an important role in the pathogenesis of GBM, particularly Fra-1.[25] The role of cFos or JunB has not been well characterized.[36–38] Here, we found that expression of cFos/JunB closely correlated with that of PGRN in S1R1 and human GBMs, and increased PGRN-downstream genes. Intriguingly, the Kaplan–Meier survival curves of the GBM cohort in Rembrandt database (http://rembrandt.nci.nih.gov) could be similarly stratified by the levels of PGRN, cFos and JunB. These results further support a mechanistic link between PGRN and cFos/JunB in GBM tumors. Finally, we investigated the mechanism of PGRN overexpression in GBM. Mutation of the AP-1 binding site attenuated PGRN promoter activity; an AP-1 inhibitor curcumin similarly reduced PGRN promoter activity, PGRN expression and its downstream genes as well.

In summary, our data indicated that PGRN overexpression in GBM could be attributed to overactive AP-1 transcription factor, and PGRN and AP-1 formed a positive feedforward loop that conferred cancer cells with growth advantage and drug resistance by activating DNA repair pathways and maintaining a pool of CSC with intrinsic drug resistance property. These results point out adding therapy, like curcumin or its derivative, targeting PGRN/AP-1 loop may significantly improve the efficacy of the current regimen for GBM cases. However, mutations in *GRN* gene cause haploinsufficiency of PGRN protein and result in a subtype of familial frontotemporal dementia characterized by atrophy of the frontal and temporal lobes of brain associated with hallmark inclusion bodies formed by TDP-43.[39] Studies of *GRN*-deficient mice revealed its importance in maintaining normal function and health of neurons in aged mice.[40,41] Thus, fine-tuning PGRN level to strike a balance between tumor inhibition and maintenance of neuronal function is essential for the success of chemotherapy targeting the PGRN/AP-1 pathway.

MATERIALS AND METHODS

GBM patients

Ten pre-collected GBM samples were provided by the Department of Neurosurgery, tissue bank of National Taiwan University Hospital in delinked fashion. The M:F ratio was 6:4. The age of diagnosis ranged from 38 to 78 years (average = 59). The protocol was approved by the Institutional Review Board, Academia Sinica.

Cell culture

GBM cell lines S1R1 and GBM8904, and HTB186 cell lines were previously described,[42–44] while the H4 cell line was obtained from American Type Tissue Culture Collection. H4 cells were maintained in DMEM and S1R1 and MCF7 in MEM/10%FBS (Invitrogen, Grand Island, NY, USA).

Lentiviral infection for knockdown and rescue

PGRN knockdown constructs TRCN0000115977, TRCN0000115979, TRCN0000115980, TRCN0000115981 were obtained from Sigma-Aldrich (St Louis, MO, USA). Rescue experiments were conducted with TRCN0000115977 against 3′ UTR of human PGRN. Lentiviral particles were produced by National RNAi Core and used at knockdown efficacy reaching 80–90%.

MTT assay

An MTT assay was performed as previously described.[45] Absorbance at $\lambda = 570$ nm was read with a VersaMax microplate reader (Molecular Devices, Sunnyvale, CA, USA). Experiments were repeated three times.

EdU assay

Cells were grown on coverslips in a 24-well dish. After appropriate treatments, DNA synthesis was assayed by EdU Imaging Kit (Life Technologies, Grand Island, NY, USA). Cells were visualized with a LSM510 confocal microscope (Carl Zeiss, Göttingen, Germany). The EDU-positive cells were manually counted.

GBM tissue array

The GBM tissue array slide was purchased from US Biomax (Rockville, MD, USA). The procedure for IHC for the tissue array slides was almost the same as described for immunofluorescence. The slides were scanned using an MIRAX scan (Carl Zeiss) by Taiwan Mouse Clinics, Academia Sinica, and the intensity of fluorescence was quantified with ImageJ (NIH, Bethesda, MD, USA).[46]

Wound healing assay

S1R1 cells were seeded in a six-well dish. Upon confluence, the dish surface was scratched with a P200 pipette tip. DMSO or 250 μM TMZ was added. The wound areas were taken and quantified at different time points.

Soft agar assay

S1R1 cells were embedded in agarose in a six-well dish at a density of 10 000 cell/well as described previously.[45] Twelve hours later, 250 μM TMZ or DMSO was added. Colony formation was monitored for 3 weeks.

Colony formation assay

Cells were seeded in 6-cm dishes at density of 6000 cells/dish and treated with 250 μM TMZ or DMSO 12 h later. Colony formation was monitored for 3 weeks. The colonies were fixed, stained with 0.1% crystal violet.

CD133 analysis by flow cytometry and cell sorter

Cells were labeled with a PE-conjugated anti-CD133 antibody as described previously (Kang and Kang, 2007) and then analyzed for CD133 expression by flow cytometry using FACScan (Becton Dickinson, San Jose, CA, USA) or sorted into $CD133^+$ and $CD133^-$ populations by an FACSAria cell sorter (Becton Dickinson).

Stem cell sphere culture

Cells were grown in ultralow attachment dishes (Corning Costar, Palo Alto, CA, USA) at a density of 4000 cells/well in medium described in

Supplementary Table 2. Two weeks later, the pictures of spheres were taken, and their size was quantified.

Unlimited self-renewal assay

S1R1 cells were seeded and maintained in ultralow attachment plates at a density of 1, 10 and 50 cells/well in 200 µl stem cell medium for 7–10 days. Each condition was replicated in 48 wells. The percentage of wells with and without spheres was recorded. Wells containing at least one neurosphere was considered as positive. The spheres were trypsinized and reseeded. The procedure was repeated for four rounds. The data collected over each round of passages were used to plot unlimited self-renewal curve, while the data from the last passage were used to calculate limiting dilution plot using ELDA (http://bioinf.wehi.edu.au/software/elda/). The experiment was repeated three times.

Differentiation assay

S1R1 cells were grown in stem cell medium in ultra-low attachment dish for ~one week. The spheres were seeded onto poly-L-Lysine-coated coverslips and cultured in stem cell medium with or without 5% FBS for 7–10 days with medium changed every 3 days.

Promoter assay

The PGRN promoter sequence was obtained from the Eukaryotic Promoter Database (http://epd.vital-it.ch), and PCR-cloned from S1R1 cells into the pGL3-basic vector (Promega, Madison, WI, USA) (Supplementary Table S1). S1R1 cells were co-transfected with pGL3-basic, pGL3-control or PGRN promoters and Renilla for 48 h. The luciferase activity was measured using a TopCount NXTTM Microplate Scintillation and Luminescence Counter (Packard Instrument, Meriden, CT, USA).

Side population analysis

The assay was performed as previously described[47] using Hoechst 1 µg/ml. One micromolar verapamil (Sigma, St Louis, MO, USA) was used as control for gating. Samples were analyzed with FACSAria cell sorter.

Cell cycle analysis

Cell cycle was analyzed as described previously[48] using an FACScan (Becton Dickinson). The cell cycle phase distribution was analyzed using FacsDiva (Becton Dickinson).

Comet assay

An alkaline comet assay was performed as previously described.[49] The slides were observed under Eclipse TE2000-U (Nikon, Tokyo, Japan). Images were captured by using a SPOT RT3 camera (Diagnostic Instruments, Sterling Heights, MI, USA) with SPOT Advance software V4.6. The Comet tail length was measured by using CometScore (TriTek Corp., Sumerduck, VA, USA).

Orthotopic xenograft studies

Mice were used in accordance with the protocol approved by the Institutional Animal Care and Use Committee. A 4- to 6-week-old NOD/SCID mouse (13/group) was mounted onto a 51600 stereotactic device (Stoelting, Wood Dale, IL, USA) and received 5×10^5 (5 µl) Sh-Control or Sh-PGRN S1R1 cells injected into the striatum at a depth of 3.5 mm and a flow rate of 1 µl/min with a syringe pump (KD Scientific, Holliston, MA, USA). Two weeks later, mice were daily injected intraperitoneally with DMSO or TMZ at 100 mg/kg for three consecutive days. Mice were weekly monitored by MRI for 6 weeks at the Functional and Micro-Magnetic Resonance Imaging Center of Academia Sinica. Ten mice/group were analyzed for survival curve.

CONFLICT OF INTEREST

The authors declare no conflict of interest.

ACKNOWLEDGEMENTS

We thank the Core Facility of the Institute of Biomedical Sciences (IBMS), National RNAi Core of Taiwan, and Taiwan Mouse Clinic for their excellent services; Dr Chen Chang and the staff Y.Y. Tung and C.M. Shih for MRI analysis, and Dr Anupam Agarwal, University of Birmingham, USA for the JunB construct. The study was funded by grants from the National Science Council and Academia Sinica of Taiwan.

REFERENCES

1 Stupp R, Mason WP, van den Bent MJ, Weller M, Fisher B, Taphoorn MJ *et al.* Radiotherapy plus concomitant and adjuvant temozolomide for glioblastoma. *N Engl J Med* 2005; **352**: 987–996.
2 Stupp R, Hegi ME, Mason WP, van den Bent MJ, Taphoorn MJ, Janzer RC *et al.* Effects of radiotherapy with concomitant and adjuvant temozolomide versus radiotherapy alone on survival in glioblastoma in a randomised phase III study: 5-year analysis of the EORTC-NCIC trial. *Lancet Oncol* 2009; **10**: 459–466.
3 Zhang J, Stevens MF, Bradshaw TD. Temozolomide: mechanisms of action, repair and resistance. *Curr Mol Pharmacol* 2012; **5**: 102–114.
4 Singh SK, Clarke ID, Terasaki M, Bonn VE, Hawkins C, Squire J *et al.* Identification of a cancer stem cell in human brain tumors. *Cancer Res* 2003; **63**: 5821–5828.
5 Galli R, Binda E, Orfanelli U, Cipelletti B, Gritti A, De Vitis S *et al.* Isolation and characterization of tumorigenic, stem-like neural precursors from human glioblastoma. *Cancer Res* 2004; **64**: 7011–7021.
6 Singh SK, Hawkins C, Clarke ID, Squire JA, Bayani J, Hide T *et al.* Identification of human brain tumour initiating cells. *Nature* 2004; **432**: 396–401.
7 Beier D, Wischhusen J, Dietmaier W, Hau P, Proescholdt M, Brawanski A *et al.* CD133 expression and cancer stem cells predict prognosis in high-grade oligodendroglial tumors. *Brain Pathol* 2008; **18**: 370–377.
8 Pallini R, Ricci-Vitiani L, Banna GL, Signore M, Lombardi D, Todaro M *et al.* Cancer stem cell analysis and clinical outcome in patients with glioblastoma multiforme. *Clin Cancer Res* 2008; **14**: 8205–8212.
9 Rebetz J, Tian D, Persson A, Widegren B, Salford LG, Englund E *et al.* Glial progenitor-like phenotype in low-grade glioma and enhanced CD133-expression and neuronal lineage differentiation potential in high-grade glioma. *PLoS ONE* 2008; **3**: e1936.
10 Zeppernick F, Ahmadi R, Campos B, Dictus C, Helmke BM, Becker N *et al.* Stem cell marker CD133 affects clinical outcome in glioma patients. *Clin Cancer Res* 2008; **14**: 123–129.
11 Zhang M, Song T, Yang L, Chen R, Wu L, Yang Z *et al.* Nestin and CD133: valuable stem cell-specific markers for determining clinical outcome of glioma patients. *J Exp Clin Cancer Res* 2008; **27**: 85.
12 Bao S, Wu Q, McLendon RE, Hao Y, Shi Q, Hjelmeland AB *et al.* Glioma stem cells promote radioresistance by preferential activation of the DNA damage response. *Nature* 2006; **444**: 756–760.
13 Kang MK, Kang SK. Tumorigenesis of chemotherapeutic drug-resistant cancer stem-like cells in brain glioma. *Stem Cell Dev* 2007; **16**: 837–847.
14 Liu G, Yuan X, Zeng Z, Tunici P, Ng H, Abdulkadir IR *et al.* Analysis of gene expression and chemoresistance of CD133+ cancer stem cells in glioblastoma. *Mol Cancer* 2006; **5**: 67.
15 Shervington A, Lu C. Expression of multidrug resistance genes in normal and cancer stem cells. *Cancer Investig* 2008; **26**: 535–542.
16 Bateman A, Bennett HP. Granulins: the structure and function of an emerging family of growth factors. *J Endocrinol* 1998; **158**: 145–151.
17 Shoyab M, McDonald VL, Byles C, Todaro GJ, Plowman GD. Epithelins 1 and 2: isolation and characterization of two cysteine-rich growth-modulating proteins. *Proc Natl Acad Sci USA* 1990; **87**: 7912–7916.
18 Donald CD, Laddu A, Chandham P, Lim SD, Cohen C, Amin M *et al.* Expression of progranulin and the epithelin/granulin precursor acrogranin correlates with neoplastic state in renal epithelium. *Anticancer Res* 2001; **21**: 3739–3742.
19 Liau LM, Lallone RL, Seitz RS, Buznikov A, Gregg JP, Kornblum HI *et al.* Identification of a human glioma-associated growth factor gene, granulin, using differential immuno-absorption. *Cancer Res* 2000; **60**: 1353–1360.
20 Pan CX, Kinch MS, Kiener PA, Langermann S, Serrero G, Sun L *et al.* PC cell-derived growth factor expression in prostatic intraepithelial neoplasia and prostatic adenocarcinoma. *Clin Cancer Res* 2004; **10**: 1333–1337.
21 Serrero G, Ioffe OB. Expression of PC-cell-derived growth factor in benign and malignant human breast epithelium. *Human Pathol* 2003; **34**: 1148–1154.
22 Cheung ST, Cheung PF, Cheng CK, Wong NC, Fan ST. Granulin-epithelin precursor and ATP-dependent binding cassette (ABC)B5 regulate liver cancer cell chemoresistance. *Gastroenterology* 2011; **140**: 344–355.
23 Wang M, Li G, Yin J, Lin T, Zhang J. Progranulin overexpression predicts overall survival in patients with glioblastoma. *Med Oncol* 2012; **29**: 2423–2431.
24 Kanzawa T, Germano IM, Komata T, Ito H, Kondo Y, Kondo S. Role of autophagy in temozolomide-induced cytotoxicity for malignant glioma cells. *Cell Death Differ* 2004; **11**: 448–457.

25 Dhandapani KM, Mahesh VB, Brann DW. Curcumin suppresses growth and chemoresistance of human glioblastoma cells via AP-1 and NFkappaB transcription factors. *J Neurochem* 2007; **102**: 522–538.
26 Frampton G, Invernizzi P, Bernuzzi F, Pae HY, Quinn M, Horvat D *et al.* Interleukin-6-driven progranulin expression increases cholangiocarcinoma growth by an Akt-dependent mechanism. *Gut* 2012; **61**: 268–277.
27 Swamydas M, Nguyen D, Allen LD, Eddy J, Dreau D. Progranulin stimulated by LPA promotes the migration of aggressive breast cancer cells. *Cell Commun Adhesion* 2011; **18**: 119–130.
28 Barazzuol L, Jena R, Burnet NG, Meira LB, Jeynes JC, Kirkby KJ *et al.* Evaluation of poly (ADP-ribose) polymerase inhibitor ABT-888 combined with radiotherapy and temozolomide in glioblastoma. *Radiat Oncol* 2013; **8**: 65.
29 Garcia-Alloza M, Borrelli LA, Rozkalne A, Hyman BT, Bacskai BJ. Curcumin labels amyloid pathology in vivo, disrupts existing plaques, and partially restores distorted neurites in an Alzheimer mouse model. *J Neurochem* 2007; **102**: 1095–1104.
30 Zhang W, Mojsilovic-Petrovic J, Andrade MF, Zhang H, Ball M, Stanimirovic DB. The expression and functional characterization of ABCG2 in brain endothelial cells and vessels. *FASEB J* 2003; **17**: 2085–2087.
31 Bleau AM, Hambardzumyan D, Ozawa T, Fomchenko EI, Huse JT, Brennan CW *et al.* PTEN/PI3K/Akt pathway regulates the side population phenotype and ABCG2 activity in glioma tumor stem-like cells. *Cell Stem Cell* 2009; **4**: 226–235.
32 Seidel S, Garvalov BK, Wirta V, von Stechow L, Schanzer A, Meletis K *et al.* A hypoxic niche regulates glioblastoma stem cells through hypoxia inducible factor 2 alpha. *Brain* 2010; **133**: 983–995.
33 Piscopo P, Rivabene R, Adduci A, Mallozzi C, Malvezzi-Campeggi L, Crestini A *et al.* Hypoxia induces up-regulation of progranulin in neuroblastoma cell lines. *Neurochem Int* 2010; **57**: 893–898.
34 Krishnamurthy P, Ross DD, Nakanishi T, Bailey-Dell K, Zhou S, Mercer KE *et al.* The stem cell marker Bcrp/ABCG2 enhances hypoxic cell survival through interactions with heme. *J Biol Chem* 2004; **279**: 24218–24225.
35 Xu Y, Stamenkovic I, Yu Q. CD44 attenuates activation of the hippo signaling pathway and is a prime therapeutic target for glioblastoma. *Cancer Res* 2010; **70**: 2455–2464.
36 Assimakopoulou M, Varakis J. AP-1 and heat shock protein 27 expression in human astrocytomas. *J Cancer Res Clin Oncol* 2001; **127**: 727–732.
37 Debinski W, Gibo DM. Fos-related antigen 1 (Fra-1) pairing with and transactivation of JunB in GBM cells. *Cancer Biol Ther* 2011; **11**: 254–262.
38 Tao T, Wang Y, Luo H, Yao L, Wang L, Wang J *et al.* Involvement of FOS-mediated miR-181b/miR-21 signalling in the progression of malignant gliomas. *Eur J Cancer* 2013; **49**: 3055–3063.
39 Rademakers R, Hutton M. The genetics of frontotemporal lobar degeneration. *Curr Neurol Neurosci Rep* 2007; **7**: 434–442.
40 Matsuwaki T, Asakura R, Suzuki M, Yamanouchi K, Nishihara M. Age-dependent changes in progranulin expression in the mouse brain. *J Reprod Dev* 2011; **57**: 113–119.
41 Filiano AJ, Martens LH, Young AH, Warmus BA, Zhou P, Diaz-Ramirez G *et al.* Dissociation of frontotemporal dementia-related deficits and neuroinflammation in progranulin haploinsufficient mice. *J Neurosci* 2013; **33**: 5352–5361.
42 Khoshyomn S, Manske GC, Lew SM, Wald SL, Penar PL. Synergistic action of genistein and cisplatin on growth inhibition and cytotoxicity of human medulloblastoma cells. *Pediatr Neurosurg* 2000; **33**: 123–131.
43 Lee PY, Chen CL, Lin ZZ, Cheng AL, Chen EI, Whang-Peng J *et al.* The Aurora kinases inhibitor VE-465 is a novel treatment for glioblastoma multiforme. *Oncology* 2013; **84**: 326–335.
44 Lin LT, Chiou SH, Lee TW, Liu RS, Hwang JJ, Chang CH *et al.* A comparative study of primary and recurrent human glioblastoma multiforme using the small animal imaging and molecular expressive profiles. *Mol Imaging Biol* 2013; **15**: 262–272.
45 Jin L, Wessely O, Marcusson EG, Ivan C, Calin GA, Alahari SK. Prooncogenic factors miR-23b and miR-27b are regulated by Her2/Neu, EGF, and TNF-alpha in breast cancer. *Cancer Res* 2013; **73**: 2884–2896.
46 Schneider CA, Rasband WS, Eliceiri KW. NIH Image to ImageJ: 25 years of image analysis. *Nat Methods* 2012; **9**: 671–675.
47 Goodell MA, Brose K, Paradis G, Conner AS, Mulligan RC. Isolation and functional properties of murine hematopoietic stem cells that are replicating in vivo. *J Exp Med* 1996; **183**: 1797–1806.
48 Lee PC, Kakadiya R, Su TL, Lee TC. Combination of bifunctional alkylating agent and arsenic trioxide synergistically suppresses the growth of drug-resistant tumor cells. *Neoplasia* 2010; **12**: 376–387.
49 Nandhakumar S, Parasuraman S, Shanmugam MM, Rao KR, Chand P, Bhat BV. Evaluation of DNA damage using single-cell gel electrophoresis (Comet Assay). *J Pharmacol Pharmacother* 2011; **2**: 107–111.

Supplementary Information accompanies this paper on the Oncogene website (http://www.nature.com/onc)